MODELLING LIQUID HYDROGEN RELEASE AND SPREAD ON WATER

Nazarpour, F.[a], Dembele, S.[c] and Wen, J.X.[b,1]
[a] School of Mechanical Engineering, Kingston University London, Friars Ave., London, SW15 3DW, United Kingdom
[b] School of Mechanical Engineering, Kingston University London, Friars Ave., London, SW15 3DW, United Kingdom
[c] School of Engineering, Warwick Fire, University of Warwick, Coventry, CV4 7AL, United Kingdom

ABSTRACT

Consequence modelling of high potential risks of usage and transportation of cryogenic liquids yet requires substantial improvements. Among the cryogenics, liquid hydrogen (LH_2) needs especial treatments and a comprehensive understanding of spill and spread of liquid and dispersion of vapor. Even though many of recent works have shed lights on various incidents such as spread, dispersion and explosion of the liquid over land, less focus was given on spill and spread of LH_2 onto water. The growing trend in ship transportation has enhanced risks such as ships' accidental releases and terrorist attacks, which may ultimately lead to the release of the cryogenic liquid onto water. The main goal of the current study is to present a computational fluid dynamic (CFD) approach using OpenFOAM to model release and spread of LH_2 over water substrate, and discuss previous approaches. It also includes empirical heat transfer equations due to boiling, and computation of evaporation rate through an energy balance. The results of the proposed model will be potentially used within another coupled model that predicts gas dispersion [1]. This work presents a good practice approach to treat pool dynamics and appropriate correlations to identify heat flux from different sources. Furthermore, some of the previous numerical approaches to redistribute, or in some extend, manipulate the LH_2 pool dynamic are brought up for discussion, and their pros and cons are explained. In the end, the proposed model is validated by modelling LH_2 spill experiment carried out in 1994 at the Research Centre Juelich in Germany [2,3].

1.0 INTRODUCTION

Applications using liquid hydrogen are growing. Although, to the best of our knowledge, there is no report of LH_2 spill on water resulting into a fatal incident, growth in applications of liquid hydrogen in future engines or power plants will increase needs to ship LH_2 in large amounts. Also, locating the power plants next to water bodies will require risk managers to understand predicted consequences of a spill incident on water. The process of such incidents includes several complex physical concepts. The utmost of spill incidents is explosion of the dispersed gas in residential or industrial environment and a great level of destruction and fatality. To predict the hazard of dispersed hydrogen explosion, the gas cloud size and its degree of concentration is required. Yet, to model dispersion, a comprehensive estimation of the pool size and evaporation rate under atmospheric conditions are needed to provide quite reliable data for further predictions.

Substantial risk in doing experiments with cryogenic liquids needs special safety conditions; therefore, most of experiments were done in small scale. For LH_2 spill, many of recent experiments were on land. Venetsanos et. Al. [3] provided a list and a review of some remarkable tests carried out in the past. Verfondern [2] reported a few of his trials run in early 90^{th}, some of which took place on water.

CFD is a fine approach to predict large incidents. However; cheaper methodologies are to be considered, as such incidents happen in large scale and the physics of the problem is rather

[1] Correspondence Jennifer.Wen@warwick.ac.uk

complex. The purpose of this paper is to present the implementation of a shallow layer theory for modelling spreading LH_2 together with energy correlation to calculate evaporation rate. The developed model is to predict the pool size, its propagation and variations of evaporation rate over release time. A similar approach has been taken by some authors [2,5,6], and implemented in quite a few available codes, such as PHAST [7,8], FLACS [6], ADREA-HF [5], and LAUV [2,3]. PHAST and LAUV used a simplified correlation of shallow water equations; FLACS and ADREA-HF are commercial codes that have also implemented the same equations, however have not given extensive details on every part of the code. In view of recent studies, questions remain on whether the codes are capable of incorporating mixing effect or how phase fraction is calculated when it comes into spill of heavy cryogenics such as N_2, and how the pool's leading edge is treated. Pool propagation decay mainly occurs due to turbulence resulting from violent evaporation environment, and to a smaller degree is caused by friction and intense evaporation at the beginning of release. A few suggested approaches [8, 9] manipulate the pool velocity that affects a realistic process, and produces high magnitude of errors within the numerical equations.

Friction is yet to be fully understood, as many have suggested different correlations with shallow clarifications on friction coefficients. In fact, propagating LH_2 over water is almost frictionless, as the liquid is considerably lighter than water and boiling film is always existent between the cryogenic pool and the water substrate. Instead, a violent boiling activity and turbulence effect especially underneath the leading edge and an inward velocity vectors can contribute to a friction coefficient in the momentum equation.

For LH_2 spill on water, in most of spilling time, the heat transfer coefficient is almost constant; however, care should be taken for convection inside small basins, as ice formation is likely to occur. Experimental observations show a sudden shrinkage of the cryogenic pool, thus, quite higher heat flux from the substrate and separation of a hydraulic jump due to spill effect from the pool. This seems to be due to boiling of the liquid in the transition regime for a very short time. The hydraulic jump is observed at initial seconds of spill time and is due to high velocity discharge of LH_2 in the low velocity zone. This leads to a rather abrupt rise in the liquid surface and propagates radially outward. LH_2 boiling point is around 20 *K*, leading to a temperature difference greater than 250 *K* during the release time. Therefore, film boiling predominantly transfers heat from the water substrate. Hence, LH_2 is sliding over a turbulent bubbly boiling film that introduces a new approach to friction. In general, within LH_2 spill on water, the cryogenic pool goes through the following process:

1- Pool propagates outward (expansion) to its maximum size just as spill takes place, due to high momentum and creation of hydraulic jump,
2- Pool stopping effects are the turbulence underneath the leading edge inside the water substrate, evaporation and boiling film friction,
3- Pool shrinks to its minimum size (contraction), due to maximum heat flux (transition boiling),
4- Pool tends to stay stationary due to film boiling during entire spill.

In summary, for a shallow layer based model, as an approximation, but remarkably cheap method to model spread and evaporation of LH_2 on water, two features are mainly recommended to be accounted for. Firstly, considering reliable correlations to calculate heat transfer coefficients. Secondly, realistic effects against pool propagation.

2.0 MODEL DESCRIPTION

The proposed model uses CFD by solving 2D shallow water equations coupled with energy equation. The code implements OpenFOAM [9] classes and libraries. It is an open-source CFD code solving continuum mechanic applications. It has been widely used and validated through many applications. Currently, OpenFOAM treats 2D models as 3D by applying the finite volume

method using numerical treatments to cancel the effect of third component. However, some features discommode the code especially when dealing with volume of fluid as faced with the current shallow layer model. An accommodating approach that implemented in our model is the finite area method that is available on OpenFOAM Extend version 3.2 and higher [10]. Finite area method solves partial differential equations by integrating over area elements instead of in volume cells. In fact, the model is purely treated 2D. Therefore, for shallow water equations every segment of area introduces a liquid height *h* and area *A*. Thus, volume of fluid is $V = h.A$. This would be subject to the height of the cell, if finite volume was implemented, and cares should have been taken for normalization of cell heights.

Figure 1 shows the parameters for discretization of finite area, where *d* is distance of the point to its neighbour, *Le* is the length edge vector and *e* stands for edge. Therefore, the flux is calculated by summation through the edges of the finite area cell.

Shallow water equations are derived from flow Navier Stokes Equations postulating that velocity component along the liquid height is too small, therefore; simplifications lead to 2-dimensioned momentum and continuity equations, where velocity components are averaged velocities. However, the effect of hydrostatic pressure is not excluded. For thin layers, such as spreading of LH_2 over water, this approach is considerably cost effective. Alternative is direct methods such as 3D volume of fluid (VOF) model that requires a quite fine mesh along the liquid depth and evaporation zone. As LH_2 release and spreading occur in large areas in high amounts, and small variations of pool size have no remarkable effect on results of dispersion models, using a direct model is not economical.

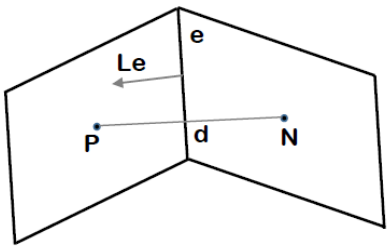

Figure 1. An example of finite area including parameters for discretization

For LH_2, it is assumed in small and stationary spills that there will be no remarkable penetration or mixing effect inside water, as liquid hydrogen is considerably lighter than water. In this case, it is a close approximation to detect LH_2 fraction readily by identifying the cell areas having $\Delta h > 0$; where $\Delta h = h - h_w$ and h_w is water depth. In instantaneous releases, this can be still the case, if the liquid height at release point is not too high. Otherwise, a phase fraction equation should be taken into consideration.

The model is capable of calculating the thermophysical properties of each element through different numerical classes, some of which are developed alongside of the main solver. Given temperatures of water substrate and ambient air, together with the releasing temperature of LH_2, all required properties are obtained through the thermophysical classes. Temperature of releasing LH_2 is assumed to remain in the saturation temperature over the entire spilling time. For confined water substrates, a 2D heat transfer model provided convection velocity magnitude. This velocity that plays an important role against pool propagating velocity was incorporated in friction factor on the right side of momentum equation.

2.1 NUMERICAL CORRELATIONS

Shallow layers momentum equations are solved based on liquid height. Density will alternatively be added to both sides of the equations, if the cryogenic liquid is not at its saturation temperature.

In most cases the release temperature is equal to the boiling temperature; therefore, density stays constant in the liquid state. The momentum and continuity equations are defined as follows:

$$\frac{\partial}{\partial t}(hU) + \nabla.(h^T hU) - g'h\nabla(h + h_0) = F_f - \dot{m}_v U + \dot{m}_{in} U + \tau_w \quad (1)$$

$$\frac{\partial}{\partial t}(h) + \nabla.(hU) = \dot{m}_{in} - \dot{m}_v \quad (2)$$

where h (m) and U (m/s) are liquid height and velocity respectively; F_f (m^2/s^2) is friction factor together with the contribution of convection velocity effect underneath LH_2 pool, $\dot{m}_v U$ and $\dot{m}_{in} U$ (m^2/s^2) account for the momentum caused by liquid release and evaporation, and τ_w is wind shear stress over the liquid surface. $\dot{m}_{in}$ and $\dot{m}_v$ (m/s) are rates of release and evaporation respectively. Rate of release depends on the duration of release and the total volume of liquid spilled. However, pragmatically liquid flow rate does not reach steady condition immediately. To model this, initial seconds of release is proportioned with a linear function by the time it arrives at steady state condition.

In Eq. (1) g' (m/s^2) is reduced gravity that is $g(1 - \rho_l/\rho_w)$; where g (m/s^2) is actual gravity acceleration, ρ_l and ρ_w (kg/m^3) are LH_2 and water densities respectively.

Vaporization rate is calculated through the following energy balance equation:

$$\frac{\partial}{\partial t}(m'H) + \nabla.(m'UH) + m'gh = Q_s + Q_w + Q_o - \dot{m}_v H_g + \dot{m}_{in} H_l \quad (3)$$

where H is specific enthalpy of LH_2 (J/kg), m' is rate of mass per area (kg/m^2), the third term on the left-side is potential energy that is to account for falling energy of release area. On the right-side Q_s (W/m^2) is heat flux from the water substrate, Q_w (W/m^2) is heat flux from atmosphere and Q_o (W/m^2) represents any other heat fluxes such as radiation or fire around the spreading pool. The two latter terms on the right-side are to consider energy loss and gain due to evaporation and release of liquid in the domain. H_g is enthalpy of the vapour hydrogen, and H_l is enthalpy of liquid as released. Calculating enthalpy, evaporation rate is obtained as follows:

$$\dot{m}_v = \frac{m'H}{H_v \rho_l dt} \quad (4)$$

where H_v (J/kg) is enthalpy of vaporization for LH_2, ρ_l is density of LH_2 (kg/m^3) and dt (s) is numerical time step.

Momentum and continuity equations are discretised on a non-uniform two-dimensional grid with a finite area method using a linear second order method over area faces that include entire area of spreading. Momentum equations are solved implicitly. Within the continuity equation, to couple with momentum equations, a Laplacian operator is to appear explicitly. However, it helps achieve better numerical stability. Sink and source mass terms are also treated explicitly. Energy equation is discretised with the same method employing a first order upwind scheme for discretization.

2.2 FRICTION FACTOR

In the previous studies, friction controls pool dynamics. FLACS implements Eq. 5 [6]; LAUV [2] included friction, but it was not mentioned what correlation was used.

$$F_f = \frac{1}{8} f_f U |\vec{U}| \quad (5)$$

In view of pool propagation, spreading starts with a hydraulic jump that forms an accelerative hump. This part has the highest velocity. Eq. 5 realistically helps to resist the hump propagation; however, there are no firm definitions on determining the dimensionless f_f coefficient. Moreover, it is unrealistic for very thin parts of the pool, where shear stress is predominant. In fact, another approach yet to be taken for regions, where pool thickness is too low to be treated as propagating pool, whereas, it is a liquid film, or a boiling film containing bubbles. Additionally, the boiling film within the film boiling regime introduces a different term to shear stress between pool and the water substrate. With this regard, [11] sums up previous works for pool spread of liquefied natural gas (LNG) inferring that it would be realistic to account for the vapour film that for LH_2 has a viscosity which is one order of magnitude lower than the liquid and three orders of magnitude lower than water viscosity. Referring to Spicer and Fay [12], assuming complete slip between the water substrate and vapour film is a straightforward approach for estimating the shear stress. This means that the water substrate is stationary and the calculated velocity is representative for the liquid thickness. Brambilla [11] suggests calculating the boiling film thickness using the following approximation:

$$\delta_{film} = \frac{\lambda_v \Delta T}{q} \tag{6}$$

where δ_{film} (m) is the boiling film liquid, ΔT (K) is temperature difference between pool and water substrate, λ_v ($W/m\ K$) is the thermal conductivity of vapour in a film temperature, and q (W/m^2) is the heat flux exchanged within the film boiling regime. The shear stress is calculated as follows:

$$\tau_{film} = \frac{\mu_v U}{\delta_{film}} \tag{7}$$

where, μ_v (kg/ms) is dynamic viscosity of vapour. Using Eq. 6, the minimum boiling film thickness for hydrogen release at 20K reaches up to 0.27 mm. This correlation was implemented in our model.

2.3 POOL FORMATION TREATMENTS

Shallow layer equations do not model breaking of hydraulic jump; it treats the flow as frictionless and non-breaking. Realistically, leading edge has the highest thickness that propagates away from the spill point. Rapid evaporation at a few initial seconds, cause the pool to shrink shortly before the leading hump breaks and hump leaves the entire pool by the time it is entirely evaporated. Webber and his colleagues [13], who made most of their contributions to LNG pool modelling, suggested the following correlation to control the pool dynamic:

$$U = \sqrt{kg(h - h_{min})} \tag{8}$$

where U is local spreading velocity of liquid (m/s), h and h_{min} (m) are the local and the minimum liquid height respectively, and g is gravitational acceleration (m/s^2). Eq. 8 is based on Bernoulli relation suggesting pool velocity at leading edge goes zero, when liquid height meets its minimum thickness. However, determining the minimum liquid height is not feasible. Furthermore, some have suggested adjusting values for k; whereas the real value for k *is 2*. Hissong [14] suggests this correlation for an integral method to calculate LNG pool size, and recommended that k value can change subject to the quality of spill point such as diffuser shape or the breach size.

In the current work, a moving boundary condition was conducted on the leading edge that reduced velocity using different minimum liquid height. Minimum possible thickness for liquid hydrogen upon its surface tension and contact angle can be estimated by puddle equations [15]. Having used it in the model, continuity error grew during the spill time. This affected the evaporation rate. The proposed solution to this was to use bounding and manipulative numerical techniques to alleviate

the error. Overall, this method is not recommended for a CFD model. Instead, it is recommended to consider three dominant effects on pool formation:

1- Pool friction due to film boiling and opposite convection velocity
2- Turbulence effect underneath leading edge,
3- Considering higher heat transfer at initial seconds of release (transition heat flux),
4- Hydraulic jump breaking effect

2.4 HEAT FLUX

LH_2 boils over water substrate. The temperature difference is higher than 250 *K*; therefore, heat transfer is mainly through film boiling. There are not many experimental researches dedicated to LH_2 pool boiling on water substrate; however, correlations resulted from a flat plate can be extended to water substrate by some considerations. An exact approach to calculate heat flux is to consider variations of water temperature during the spill. Especially for small confined water basins, ice formation changes the heat flux scenario. Maximum heat flux at saturation temperature occurs shortly before boiling enters transition regime. For LH_2 boiling on water this might happen just at the beginning. Shirai et al. [16] predict critical heat flux using the curve of Kutateladz's equation with the coefficient of 0.16 for pressures from 0.11 to 1.1 *MPa* under saturated conditions. This gave a good agreement with his experimental data:

$$q_{cr} = 0.16 H_v \rho_v \left[\frac{g\sigma(\rho_l - \rho_v)}{{\rho_v}^2}\right]^{1/4} \tag{9}$$

where H_v (*J/kg*) is hydrogen enthalpy of evaporation, ρ_v and ρ_l (kg/m^3) are density of vapour and liquid hydrogen respectively, σ is surface tension (*N/m*), and g (m/s^2) is gravitational acceleration. For LH_2 at temperature of about 20.36 K, q_{cr} is around 90 KW/m^2. Minimum heat flux can be obtained by Zuber correlation [17] as follows:

$$q_{min} = H_v \rho_v \left(\sigma g \frac{\rho_l - \rho_v}{\rho_v^2}\right)^{1/4} \left(\frac{\rho_l}{\rho_l + \rho_v}\right)^{1/2} \tag{10}$$

The difference between maximum and critical heat fluxes is not high. As boiling is predominantly in film boiling regime, heat flux changes from 80 to 100 KW/m^2. This agrees well with Verfondern and Dienhart selected temperature for LAUV code [2].

Atmospheric heat flux was included in this model in a way explained by Hissong [14] for LNG. The following correlation is for an unignited pool:

$$q_a = h_a A_t (T_a - T_{LH2}) \tag{11}$$

where h_a is atmospheric heat transfer coefficient (W/m^2K), A_t is pool area varying at each time step (m^2), T_a and T_{LH2} are atmospheric and LH_2 temperature (*K*). In the CFD model heat flux of both substrate and atmosphere are calculated in every finite area respectively. It adapts the model for varying substrate's temperature in small basins, where ice formation is likely to happen. Therefore, A_t is summation of all areas that contain liquid. Density of LH_2 is much smaller than water density, Verfondern [2,3] observed that only 7% of LH_2 is below the water surface. Therefore, it can be assumed that the spilling LH_2 flows over water surface. Furthermore, if water surface is calm, in a confined basin, LH_2 spread is almost frictionless. If the water substrate is wavy the effect of wave dominantly control pool propagation.

Atmospheric heat transfer coefficient (h_a) is calculated as follows [14]:

$$h_a = \frac{Nu\ \lambda_a}{D_t} \tag{12}$$

where λ_a is air thermal conductivity (W/mK), D_t is pool diameter at each time step, which was defined as the diagonal of 2D area cell in the model. Nu is Nusselt number that is obtained as follows [18]:

$$Nu = 0.037\ Re^{0.8} Pr^{1/3} \tag{13}$$

where Re and Pr are Reynolds and Prandtl number that are defined below:

$$Re = \frac{D_t U_w}{\nu_a} \tag{14}$$

$$\mathrm{Pr} = \frac{C_{pa}\mu_a}{\lambda_a} \tag{15}$$

where U_W is velocity of wind at 10 m height (m/s), and ν_a is atmospheric kinematic viscosity at the average temperature of LH_2 and ambient temperature. (m^2/s), C_{pa} is air heat capacity ($J/kg\ K$), μ_a is air dynamic viscosity ($Pa.s$), and λ_a is air thermal conductivity that all are calculated at the average temperature of LH_2 and ambient temperature.

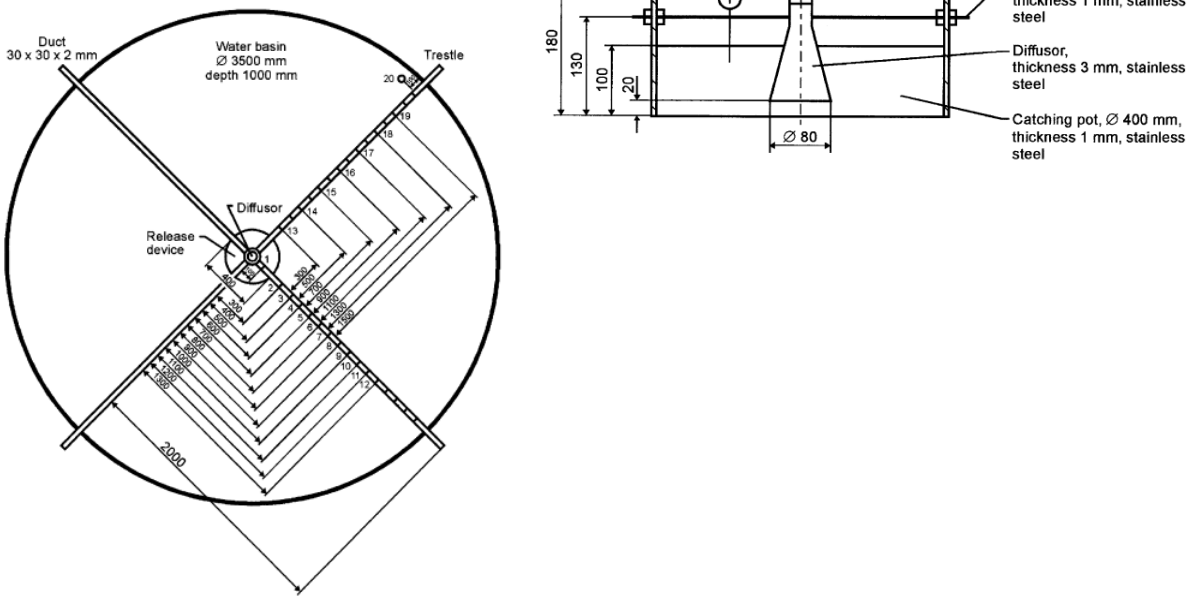

Figure 2. Experimental arrangement of LH2 spill on water substrate [2]

3.0 RESULTS AND DISCUSSION

The proposed model has been validated using an experiment carried out in 1994 at the Research Centre Juelich (FZJ) in Germany. Details of the experiments reported by Verfondern and Dienhart [2,3], where they also validated their trial results introducing LAUV code [19]. Experiment was from a

series of test studies focused on understanding and predicting the risks and consequences of accidental release of cryogenic liquids over ground and water. Two of the tests focused on LH_2 spill on water substrate that were all reported in one figure showing the pool size variations obtained by the installed thermocouples and observing video-recordings. However, Verfondern [2] explains that the LH_2 pool propagated beyond the covered range of thermocouples and the coverage of video recordings. He pointed out that considerably low kinematic viscosity of hydrogen certainly influenced the stability of the pool's leading edge and its breakup. He mentioned a sort of pulsation behaviour that caused the pool to propagate unsymmetrically.

3.1 EXPERIMENTAL CONDITION

LH_2 spill experiment over water substrate was carried out in a confined water basin, whose diameter was 3.5m. This was filled with 1m of water depth. Figure 2 shows a schematic picture of the experiment's arrangement, as given by Verfondern [2]. 18 thermocouples were positioned approximately 1mm above the surface of the ground along with rods extended cross-shaped on the top of the water basin. The thermocouples' measurements data were reported on pool size variations during the spill time. Seemingly, these were also used for measuring thermal variations inside the water basin during spill; however, no such results were reported. LH_2 was spilled from an 80mm diffuser onto water perpendicular to the water surface for 62 seconds with a flow rate of about 0.005 m^3/s.

Ice formation was clearly reported, as during spill a single small floe escaped outward the pool area, and after cutting off the source, a massive ice layer was observed over the pool boiling region. Also long-shaped ice tracks that led radially away could be observed.

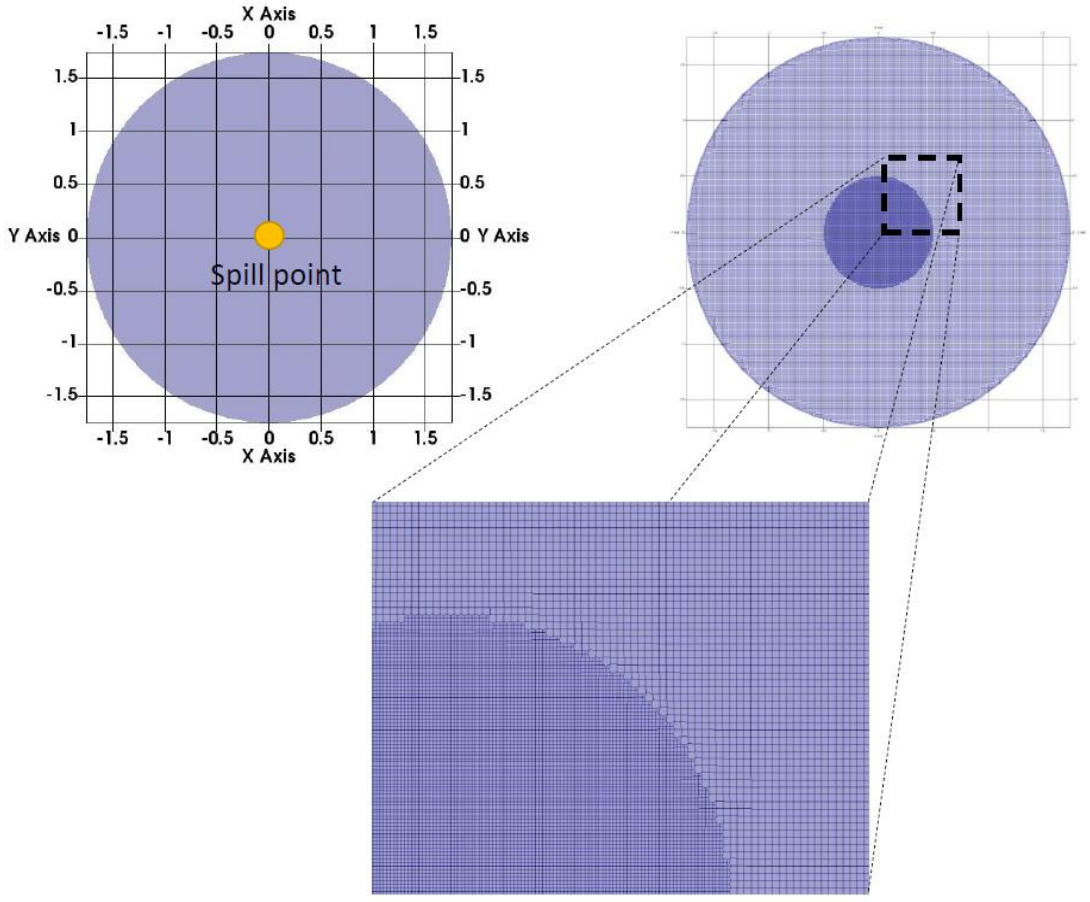

Figure 3. Numerical mesh arrangement

3.2 NUMERICAL SET-UP

Figure 3 shows the numerical mesh. It was rather finer around the releasing point as well as where the pool is formed. This was due to establishment of high gradient of liquid height especially around the spill point. Earlier numerical trials with coarser mesh yielded instabilities started by sudden raise of courant number and producing unrealistic velocity results. This 2D rectangular mesh was prepared in OpenFOAM and used for the proposed finite area solver. This had around 150000 area cells. The mesh performance in accordance with numerical schemes was unconditionally stable. Choosing a small time-step and relatively higher number of correction (~6-10) for continuity equation were required, as, otherwise, even continuity errors with small residuals are accumulated into large errors. This would be contributed to the evaporation rate. In this case, evaporation rate surpasses the actual spilled volume of LH_2.

3.3 RESULTS

Figure 4. shows results of the proposed model together with scattering positions of pool's leading edge obtained by thermocouples from two different branches of the cross-shaped rods. Test results clearly show of a remarkable expansion at first two seconds. This is due to high releasing momentum and formation of a hydraulic jump. Afterwards, pool shrinks due to high evaporation rate that pertains to critical heat flux and passing over the transition boiling regime. Eventually, pool will tend to arrive at a stationary condition with film boiling regime. Even though the temperature difference between these two early stages is rather small (~10 KW/m^2), its influence on the pool size is remarkable.

Considering the results of the proposed model, it predicts a circular pool (see figure 1) with a considerably close size to what measured in the experiment. Comparing with LAUV predictions, our proposed model has slightly closer predictions to the experiment.

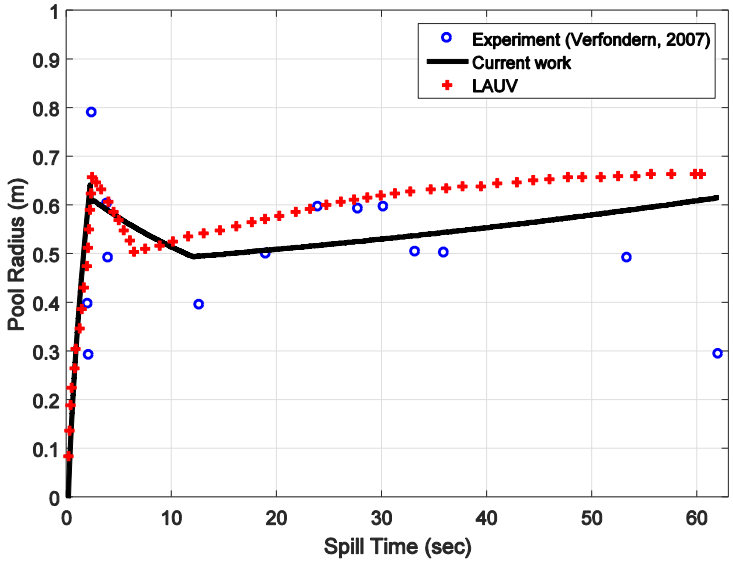

Figure 4. Pool size variation during spill for 62 s, 5 l/s, compared with test results and LAUV code

Figure 5 shows pool formation shortly after spill. Hydraulic jump is created and rapidly propagates outward as much it reaches its maximum size. The figure shows, due to evaporation, the pool breaks up and the propagating hump leaves the pool and is evaporated soon after. Afterwards, pool leading

edge velocity remains in a rather small range and controlled by evaporation rate. Considering pool height variations given in figure 5, minimum pool height always is larger than boiling film that is obtained from Eq. 6. Results show that average pool height is generally so small that agrees with experimental observations showing that liquid pool is largely engulfed with a vapour cloud. Average evaporation rate was 0.072 kg/sm^2 and average heat flux from water substrate ranged from 80 - 96 KW/m^2. Calculation of atmospheric heat flux calculated by Eq. 11 is shown in figure 6. The average heat flux from ambient air reaches to 5.5 KW/m^2 It is rather higher than 0.5 KW/m^2 that was suggested by Verfondern and Dienhart [2,3]; however, incorporation of both substrate and atmospheric heat flux agrees with LAUV model.

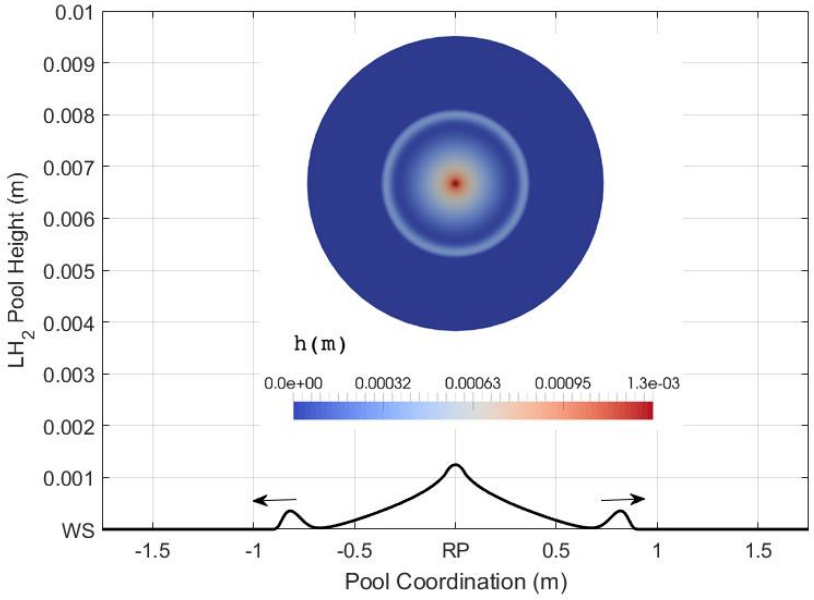

Figure 5. Propagating pool by the time the hydraulic jump leaves the pool. RP stands for release point and WS is for water surface

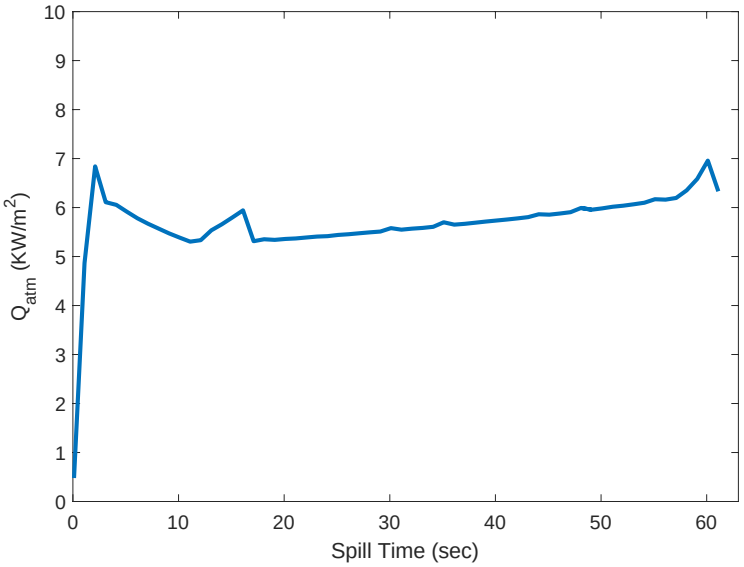

Figure 6. Variation of atmospheric heat flux during spill time

The effect of velocity underneath the pool was also included together with the friction factor. Figure 7 shows simulation of convection heat transfer inside a water basin underneath a developed

LH_2 pool. Simulation was based on a 2D Boussinesq heat transfer model to do inceptive studies on velocity magnitudes around the pool. The model shows appearance of high velocity and development of turbulent velocities underneath the pool leading edge. The opposite effect of velocity vectors was incorporated in the momentum equation.

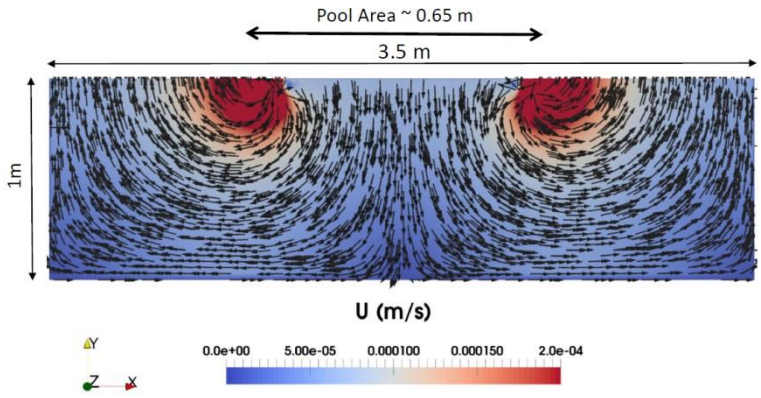

Figure 7. Velocity of water inside the water substrate and underneath the propagating LH_2 pool due to convection and LH2 pool formation. Red zones are the leading edge areas, where turbulence causes pool stopping

4. CONCLUSION

A CFD code, developed in OpenFOAM [10] was used to investigate LH_2 pool size during spilling on water. Shallow water equations together with an energy balance equation were solved to predict pool height, size and evaporation rate during spill. Finite area approach benefits the model for more improved stability. It will be also beneficial for further coupling of this model with a 3D dispersion model. Recent approaches in determining factors controlling pool dynamic were incorporated in the model. Among these, the effect of convection velocity acting beneath LH_2 pool was found remarkable and was implemented in the friction factor. Controlling pool dynamic by adjusting empirical correlations over the leading edge caused erroneous results.

Verifications were made by comparing the results with experimental measurements conducted in a release test of LH_2 on water at the German Research Centre Juelich (FZJ) in 1994. Results show of close agreement with measurements, and pool size changes obtained from the model agrees with heat flux variations at early stages of release. This model is extensively valid for other cryogenic liquids such as N_2, CH_4 and even mixed liquids such as liquefied natural gas (LNG). This will be presented in further publications.

ACKNOWLEDGMENTS

This research is part of a larger research project dedicated for safer production and transportation of cryogenic liquids. This project is supported and financed by the European Commission, Marie Curie Actions.

5. REFERENCES

1. Nazarpour F., Wen J., Dembele S., Udechukwu I. D., LNG Vapour Cloud Dispersion Modelling and Simulations with OpenFOAM, *Journal of Chemical Engineering Transactions,* **48,** 2016, pp. 967 – 972.
2. Verfondern K., Dienhart B., Pool Spreading and Vaporization of Liquid Hydrogen, *International Journal of Hydrogen Energy*, 2007, **32**, pp. 2106 – 2117.
3. Verfondern K., Dienhart B., Experimental and Theoretical Investigation of Liquid Hydrogen Pool Spreading and Vaporization, *International Journal of Hydrogen Energy*, 1997, **22**, No. 7, pp. 649 – 60.
4. Venetsanos, A.G., Bartzis, J.G., CFD Modelling of Large-Scale LH_2 Spills in Open Environment, |*International Journal of Hydrogen Energy*, **32**, 2007, pp. 2171 – 2177.
5. Venetsanos, A.G., Papanikolaou, E. and Bartzis, J.G., The ADREA-HF Code for Consequence Assessment of Hydrogen Applications, *Journal Hydrogen Energy*, **35**, 2010, pp. 3908 – 3918.
6. Middha, P., Ichard, M., and Arntzen, B.J., Validation of CFD Modelling of LH_2 Spread and Evaporation against Large-Scale Spill Experiments, *Journal of Hydrogen Energy*, **36**, 2011, pp. 2620 – 2627.
7. Witlox, H., PVAP- Theory document. *London: DNV Software* (Phast 6.7 Technical Reference Documentation), 2006.
8. Webber, D. and Witlox, H, PVAP- Verification document. *London: DNV Software* (Phast 6.7 Technical Reference Documentation), 2003.
9. Weller, H.G., Tabor, G., Jasak, H., Fureby, C., A Tensorial Approach to Computational Continuum Mechanics Using Object-Oriented Techniques, *Journal of Computer in Physics*, **12**, 1998, No. 6.
10. OpenFOAM Extend Project Version 3.2 – 4.0, www.foam-extend.fsb.hr.
11. Brambilla, S., Manca, Accidents Involving Liquids: A Step Ahead in Modelling Pool Spreading, Evaporation and Burning, *Journal of Hazardous Materials*, **161**, 2009, pp. 1265 – 1280.
12. FERC Commission, Notice of Availability of Staff's Responses to Comments on the Consequence Assessment Methods for Incidents Involving Releases from Liquefied Natural Gas Carriers, Docket No. AD04-6-000, 2004.
13. Webber DM., Source terms, *Journal of Loss Prevention in the Process Industry*, 1991, No. 4, pp. 5 – 15.
14. Hissong, D.W., Keys to Modelling LNG Spills on Water, *Journal of Hazardous Materials*, **140**, 2007, No. 3, pp. 465 – 477.
15. De Gennes, P.G., Brochard-Wyart, F., Quéré, D., Capillary and Wetting Phenomena—Drops, Bubbles, Pearls, Waves, *Alex Reisinger, Springer, 2004*, ISBN 0-387-00592-7.
16. Shirai, Y., Tatsumoto, H., Shiotsu, M., Hata, K., Kobayashi, H., Naruo, Y., Inatani, Y., Boiling Heat Transfer from a Horizontal Flat Plate in a Pool of Liquid Hydrogen, *Cryogenics Journal*, **50**, 2010, pp. 410 – 416.
17. Zuber, N., Hydrodynamic Aspects of Boiling Heat Transfer, *PhD thesis, University of California*, June 1959. United States Atomic Energy Commission.
18. Incropera, F.P., DeWitt, D.P., Fundamentals of Heat and Mass Transfer, 5th ed., Wiley, Hoboken, NJ, 2002, p. 397.
19. Dienhart B., Ausbreitung und Verdampfung von fluessigem Wasserstoff auf Wasser und festem Untergrund, *Research Center Juelich Report*, No. Juel-3155, 1995.